Available online at www.sciencedirect.com
ScienceDirect
Journal of Power Sources 170 (2007) 425–432
JOURNAL OF POWER SOURCES
www.elsevier.com/locate/jpowsour

Enhanced electrochemical properties of nanocomposite polymer electrolyte based on copolymer with exfoliated clays

Mingkui Wang *, Shaojun Dong **

State Key Laboratory of Electroanalytical Chemistry, Changchun Institute of Applied Chemistry, Chinese Academy of Sciences, Changchun 130022, China

Received 13 September 2006; received in revised form 10 April 2007; accepted 15 April 2007
Available online 22 April 2007

Abstract

In this present work, a polymer electrolyte based on polymer/clay nanocomposite has been developed. Montmorillonite (MMT) clay was used as the filler, due to its special size in length and thickness, and its sandwich type structure. The obtained gel polymer electrolytes have high ionic conductivity up to 2.5 mS cm^{-1} with high cationic transference number (about 0.64) at room temperature. The influences of the filler on the membrane morphology, the solvent uptake, the ionic conductivity, and the cation transport number were investigated, and thus the significant contribution from the exfoliated organophilic MMT was identified.

Keywords: Nanocomposite; Polymer electrolyte; Ionic conductivity; Impedance spectroscopy; Lithium battery

1. Introduction

Polymer electrolytes have received considerable attention due to the vast application potential in advanced electrochemical devices, such as high energy density batteries [1,2]. In batteries, polymer electrolytes are used not only as the electrolytes, but also as the separators between the anode and the cathode. Therefore, polymer electrolytes should have high ionic conductivity, good dimensional stability, and high electrochemical stability. And even more, as the materials to be used in a large-scale battery production, the bulk polymers have to meet more requirements: (I) wide electrochemical window, (II) good compatibility with salt, (III) sufficient thermal stability, (IV) processable ability, and (V) good mechanical stability. Recently, several composite polymer electrolytes (CPEs) with high ionic conductivity based on poly(ethylene oxide), poly(methyl methacrylate), and poly(vinylidene fluoridehexafluoro-propylene) (PVDF-HFP) [3-6] have been reported. Especially, CPEs based on PVDF-HFP with inorganic fillers have been extensively studied [7]. The copolymer PVDF-HFP has a very low crystallization at room temperature (RT), and meets most requirements in terms of electrochemical performances, process-ability and safety. Many research reports show the inorganic fillers in nanometer scale or organic plasticizer can largely increase the CPEs ionic conductivity [7,8]. The addition of inorganic fillers or organic plasticizers can prevent the polymer crystallization, and thus promotes the ions transportation in the morphology phase and also improves the interfacial electrochemical stability. However, in those CPEs systems the cationic transference number is relative low (about 0.2–0.4) [9]. Many research interests were put on the methods to increase the cationic transference number by using single ionic polymer electrolytes [10,11] or addition anion receptors [12].

In addition, nanocomposites based on polymer/clay systems have also attracted considerable interests in order to develop new materials with structural and functional advantages over the conventionally reinforced polymers [13,14]. Montmorillonite (MMT) clays contain stacked silicate sheets measuring ∼10 Å in thickness and ∼2800 Å in length, which are mostly used as the inorganic host in the polymer nanocomposite field [15]. MMT clays are 2:1 charged phyllosilicates that contain exchangeable interlayer cations. The silicate sheets present a number of interesting properties such as cationic exchange capacity, intercalation, and swelling [14]. Especially, the high swelling

* Corresponding author. Present address: Laboratory of Photonics and Interfaces, Institute of Chemical Sciences and Engineering, Ecole Polytechnique Fédérale de Lausanne, 1015 Lausanne, Switzerland. Tel.: +41 21 6934944; fax: +41 21 6934111.
** Corresponding author. Tel.: +86 431 5261011; fax: +86 431 5689711.
E-mail addresses: mingkuiw@yahoo.com (M. Wang), dongsj@ns.ciac.jl.cn (S. Dong).

0378-7753/$ – see front matter © 2007 Elsevier B.V. All rights reserved.
doi:10.1016/j.jpowsour.2007.04.031

capacity of MMT is significant for the efficient intercalation of organic species, including polymers. The intercalation of polymer into clays can combine the organic guest (polymers) and the inorganic host (clays) into a single material. The resulted materials not only have the optical and electrical properties of the guest polymer, but also the mechanical strength, thermal stability, and electronic properties of the inorganic host. So the composites possess properties that may not be achieved by either component separately [14]. Generally speaking, there are two terms used to describe the prepared polymer/clay nanocomposite: intercalated and delaminated nanocomposite. In the intercalated structures case, the MMT clays sustain the self-assembled, well-order multi-layer structures. The extended polymer chains are inserted into the gallery space between parallel individual silicates layers. In the delaminated structures case, the interlayer spacing can be on the order of the radius of gyration of the polymer. The individual silicate layers are no longer close enough to interact with the adjacent layers' gallery cations when the delaminated (or exfoliated) structures could be obtained. Therefore, the silicate layers may be considered to disperse in the organic polymer. Thus the nanocomposite has a monolithic structure in micro-scale [16]. It should lead to most dramatic changes in mechanical and physical properties of the new materials.

Many related works used polymer/clay nanocomposite in solid-state electrolytes [17–19]. The intercalated or exfoliated state of MMT plays a distinct role on the ion conduction in these electrolytes [18,19]. A completely exfoliated morphology is expected to yield the highest ionic conductivity since more cations could be mobile and available for conduction. Conversely, those systems, in which cations are "trapped" between the intercalated platelets, would not be nearly considered as good ionic conductors [19]. In this present work, a polymer electrolyte based on polymer/clay nanocomposite was developed. In order to avoid the "pillar effect" in the intercalation nanocomposite, the exfoliated organophilic MMT clay disperse into polymer PVDF-HFP [19]. The large clay platelets could have a role as anions and have a low mobility because of their large size. The effects of fillers on the ionic conductivity and the cationic transport number are particularly discussed. A Li-ion polymer battery was also prepared to evaluate the polymer electrolyte performance.

2. Experimental

2.1. Materials

Battery-grade lithium hexafluorophosphate ($LiPF_6$), ethylene carbonate (EC), and dimethyl carbonate (DMC) were obtained from Merck and used as received. PVDF-HFP copolymer (Kynar Flex® 2801, $M_w = 477{,}000\ g\ mol^{-1}$) was purchased from Alf-Atochem. Hexadecyl trimethyl ammonium bromide ($C_{16}H_{33}N(CH_3)_3Br$) and dimethyl formamide (DMF) were obtained from Aldrich. The MMT clays (Magnesium Lithium Phyllosilicate Mineral) were kindly supplied by American Colloid Company with no cation-exchange capacity value given and used as received. The chemical formula of the clay is naturally occurring hydrated silicate mineral of sodium, calcium, magnesium, and lithium. The electrode materials are meso-carbon micro-beads (MCMB, ShangHai ShanShan Ltd., China) and $LiCoO_2$ (Guanyu Ltd., China).

2.2. Preparation of the polymer clay nanocomposites and GPEs

The organophilic MMT was prepared according to the previous work [18]. The polymer membranes were made with the solvent casting method. All percentages for the additives were normalized with respect to the weight of the polymer. Typically, a procedure involved 3 wt.% organophilic MMT loading was prepared as following. First, organophilic MMT (0.03 g) powder was introduced into 10 ml of DMF solution with stirring for 12 h at RT. PVDF-HFP powders (0.97 g) were added to DMF solution (10 ml) in another glass bottle with stirring for 12 h at 80 °C. Second, the clay solution was mixed with the polymer solution with shear supplied via sonication for 24 h at 60 °C. The resulted viscous slurry was cast onto a glass substrate using a doctor blade and slowly dried at 60 °C, until a uniform and freestanding membranes was gotten. And finally, the membranes were punched into circular pieces and dried at 60 °C in a vacuum oven (10^{-2} Torr) for 24 h before use.

GPEs were prepared by immersing the membranes into a liquid electrolyte solution, such as 1 M $LiPF_6$ in EC:DMC = 1:1, for a period of time. The membrane swells quickly and its weight increases significantly. The percentage of solvent uptake (η) was calculated by the following formula:

$$\eta = \frac{W_t - W_0}{W_0} \times 100\% \quad (1)$$

where W_0 and W_t are the weight of the dry members before and after absorbing liquid electrolyte within a regular time at RT.

All preparations and measurements of samples were made in an argon glove box (M. Braun, GmbH, Germany) containing less than 1 ppm H_2O.

2.3. Preparation of electrodes

The carbon anode was prepared by coating slurry of MCMB, PVdF-HFP, super-P carbon and *N*-methyl-2-pyrrolidinone (NMP) on to a copper foil. The cathode was a mixture of $LiCoO_2$, PVdF-HFP and acetylene black, which was cast on to aluminum foil. The electrodes were dried at 110 °C overnight under vacuum. The electrodes were roll-pressed under an appropriate pressure to obtain uniform thickness. The active mass loading was adjusted to have a capacity about 3.0 mAh cm^{-2}. The anode and cathode electrodes were punched into discs with an area about 0.785 cm^2 and stored in the glove box.

2.4. Measurements

Wide angle X-ray scanning (WAXS) diffraction study of the polymer/clay nanocomposite was conducted with a Rigaku D/Max 2500V PC X-ray diffractometer with copper target and Ni filter at a scanning rate of $1^\circ\ min^{-1}$.

Transmission electron microscopy (TEM) was used to observe the morphology of the samples on a JEOL 2010 system operated at an accelerating voltage of 160 kV. Samples for TEM characterization were prepared with a diamond knife on a microtome at RT to give sections with a nominal thickness at around 70 nm. The sections were transferred from water to carbon coated copper grid and dried at room temperature.

The "intrinsic" conductivities of the neat liquid electrolytes were determined directly using a conductivity meter (model DDSJ-308A, Shanghai LeiCi Ltd., China), whose cell constant was pre-calibrated by a standard KCl solution. The ionic conductivity of GPEs at temperatures ranging from −5 to 60 °C was estimated from the ac electrochemical impedance spectroscopy (EIS) results. The GPES were sandwiched between two stainless steel (SS 304) electrodes within a laboratory built Teflon cell [11]. The GPEs membranes have the thickness about 50–150 μm and area about 0.785 cm^2. The ac impedance was measured with an Autolab Frequency Response Analyzer setup consisting of Autolab PGSTAT 30 (Eco Chemie, The Netherlands) and FRA module with a fit and simulation software for the analysis of the impedance data. The EIS measurements were measured under an oscillation potential of 10 mV with a frequency range of 0.005 Hz to 1 MHz.

The stability of the lithium electrode and polymer electrolyte interface was evaluated by measuring the ac impedance response of a Li/GPE/Li cell under open circuit potential condition, which was stored at 22 °C. The change of the impedance was continuously monitored after the cell assembly.

The method proposed by Bruce and Vincent was used for the determination of the transference number, t_{Li^+} of Li^+ ions [20]. The assembled cell was kept at 25 °C for 24 h before the transference number determinations were carried out.

The charge and discharge cycling test of a $LiCoO_2$/GPE/MCMB battery was conducted between 2.8 and 4.2 V with a battery testing system (Zhenfan Electron Co. Ltd., China).

3. Results and discussion

Sonication is a good method to aid the delamination process and prepare the polymer/clay nanocomposite [21]. In this present work, PVDF-HFP/organophilic MMT clay suspensions were sonicated to enhance the clays delamination. In order to make the hydrophobic polymer easily intercalate into the hydrophilic MMT layers, the clays should be treated with organophilic reagents. Lan et al. have reported that the alkyl-ammonium ions with chain length larger than eight carbon atoms were favoring the preparation of the delaminated nanocomposite [22]. In our work, the organophilic MMT clays were obtained by the cationic exchanging between the cations in the MMT and hexadecyl trimethyl ammonium cations of the intercalating agent [18]. WAXS measurements can be used to characterize the resulted nanocomposite structure. The WAXS patterns of the air-dried MMT powders before and after treated with the intercalating agent are presented in Fig. 1a and b. The main MMT (0 0 1) diffraction reflections are obtained in both samples. Untreated MMT clays do not undergo the gallery expansion. Once treated

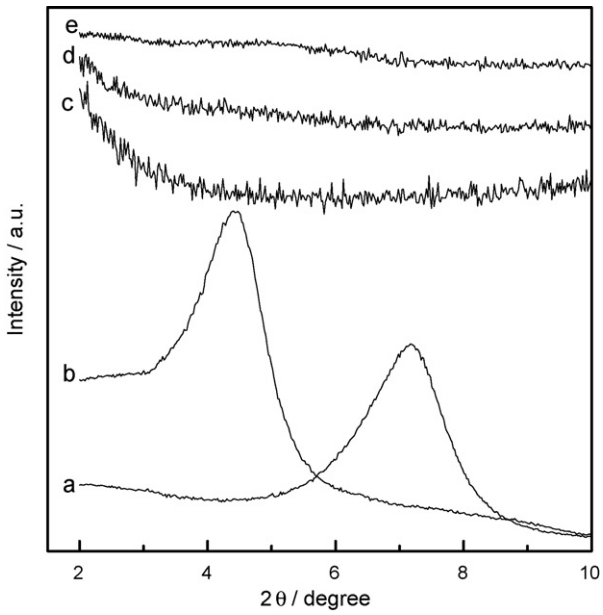

Fig. 1. WAXS patterns of (a) MMT powder, (b) organophilic MMT powder, (c) PVDF-HFP powder, (d) polymer/clay nanocomposite film (2 wt.% organophilic MMT), and (e) polymer/clay nanocomposite film (4 wt.% organophilic MMT).

with the intercalating agent, the sample shows the (0 0 1) diffraction reflection changes from 7.1° to 4.5°, i.e., the basal spacing d expands from 1.23 to 1.997 nm, indicating the incorporation of alkylammonium ions. The polymer has low crystallization as shown in Fig. 1c. The delamination of MMT layers was further improved by the sonication the samples in DMF. The spacing d increases with the sonication time, which can be evaluated from the shift of the XRD peak to smaller 2θ angles. The WAXS patterns for the dried polymer/clay nanocomposite films (2 and 4 wt.%) processed via sonication (24 h) show the loss of the low angle peak at 4.5° in Fig. 1d and e, respectively, indicating that the exfoliation exists in these two composite materials. XRD analysis alone is not enough to interpret the extent of the exfoliation. Thus, TEM studies are necessary to verify the extent of exfoliation achieved. As presented in Fig. 2, TEM image reveals that there is a mixed nanomorphology in the polymer/clay nanocomposite material with 4 wt.% clay loading.

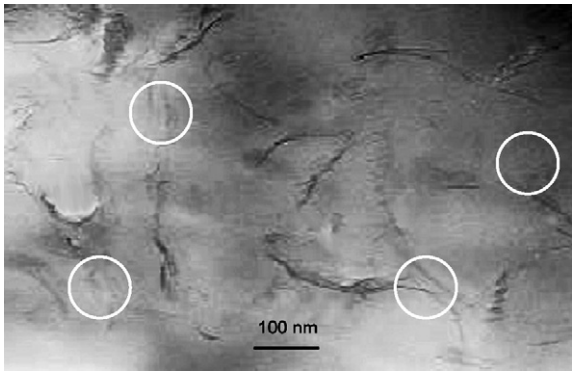

Fig. 2. TEM image of a nanocomposite electrolyte with 4 wt.% organophilic MMT dispersed in PVDF-HFP. The circled regions identify the exfoliated MMT platelets.

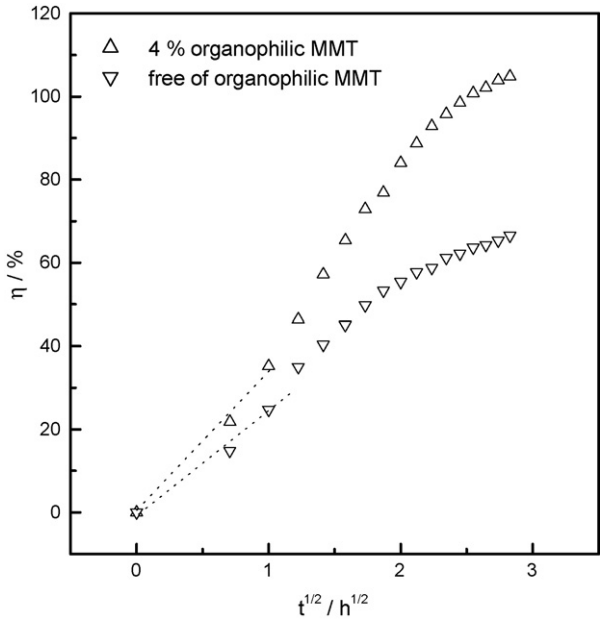

Fig. 3. The relationship of EC:DMC solvent uptake percentage vs. the square root of time for the polymer films with organophilic MMT (△) and without organophilic MMT (▽).

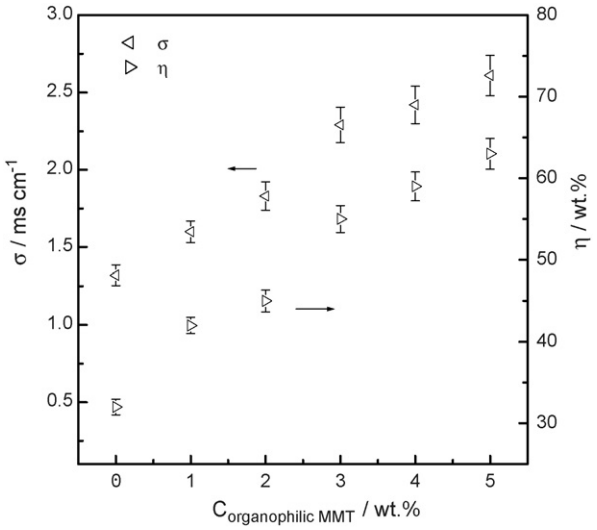

Fig. 4. The organophilic MMT content in GPEs dependence of the ionic conductivity σ (left ordinate) and the electrolyte uptake η (right ordinate) at RT. Error bars indicated the deviation of five repetitive determinations.

Individual silicate layers (as pointed in the circuits), along with two and three-layer stacks, are found to be exfoliated in the PVDF-HFP matrix. The platelets have a thickness about 3 nm and length about 250 nm. In addition, some large intercalated tactoids can also be observed.

The polymer/clay nanocomposite exhibit very good film formation and dimensional stability. Most importantly, the membrane containing the exfoliated MMT shows excellent wettability with the electrolyte solution, owning to the high surface area of the silicates layers and good affinity of PVDF to the organic electrolyte solution. The solvent uptake of polymer membrane containing the exfoliated MMT increases largely comparing with those without the filler in the same time scale. Fig. 3 presents the solvent uptake percentage of the different films as the function of the square root of time, which is used to adsorb the solvent. The percentage can be calculated according to Eq. (1). The results illustrate the percentage increases to nearly 40 wt.% in 1 h for the membranes containing the exfoliated MMT. At first part the curve is linear as illustrated in Fig. 3, which has the characteristic of Fickian diffusion [23]. As the swelling ratios increasing, the diffusion becomes anomalous, and the curve shape becomes sigmoidal. As shown in Fig. 4 (right ordinate), the solvent uptake percentage increases with the content of organophilic MMT in the membranes within 2.5 h. The result suggests that organophilic MMT facilitates solvent uptake. The solvent uptake percentage of these GPEs was fixed by control of the immersing time.

EIS analysis was further performed to understand the ion conduction in GPEs. Fig. 5 presents the typical impedance spectroscopy curves in Cole–Cole form. The samples were the nanocomposite polymer electrolytes, which were measured before and after gelling with liquid solvents. All the samples in Fig. 5 have the same organophilic MMT content (3 wt.%). As illustrated in Fig. 5a, a semicircle starts from the origin of the plot in the high-frequency range followed by a straight line inclined to the real axis in the low-frequency range. The diameter of the semicircle decreases after the membrane impregnated with 40 wt.% EC/DMC solution (see Fig. 5b). Both of the results show the capacitive behavior at the higher frequency range in the two systems. The low ionic conduction character is the insulating behavior of both the organic guest and the inorganic host matrix, because all the valence electrons are involved in the bonds that sustain their structure. The impedance spectrum of GPEs (membranes impregnated with 1 M $LiPF_6$ in EC/DMC solution) describes an approximately straight line starting from the real axis (see Fig. 5c). The disappearance of semicircular portion in the high-frequency range as shown in the inset of Fig. 5c suggests that the current carriers are ions according to the theoretical analysis [24]. We use a single $(R_bCPE_g)(R_{ct}CPE_{dl})$ circuit to describe the ac response [18,24]. R_b and R_{ct} represent the resistance of bulk electrolyte and charger transfer between the electrolyte and the blocking electrodes. Constant phase elements CPE_g and CPE_{dl} may be associated with the bulk electrolyte and the double-layer capacitances of the interface between the electrolyte and the blocking electrodes, respectively. The constant phase element was necessarily introduced to account for the non-ideality of the interface between the electrode and electrolyte [25].

Hence, the resistance R_b can be estimated. The ionic conductivity of the GPE is calculated by:

$$\sigma = \frac{l}{AR_b} \tag{2}$$

where σ is the ionic conductivity, l the thickness of the polymer electrolyte film, and A is the area of the SS electrode, respectively.

The affinity between lithium salts and PVDF-based polymer is very poor, so polar solvent (or plasticizer) should be added in GPEs systems [11,18,26]. EC and DMC were used in

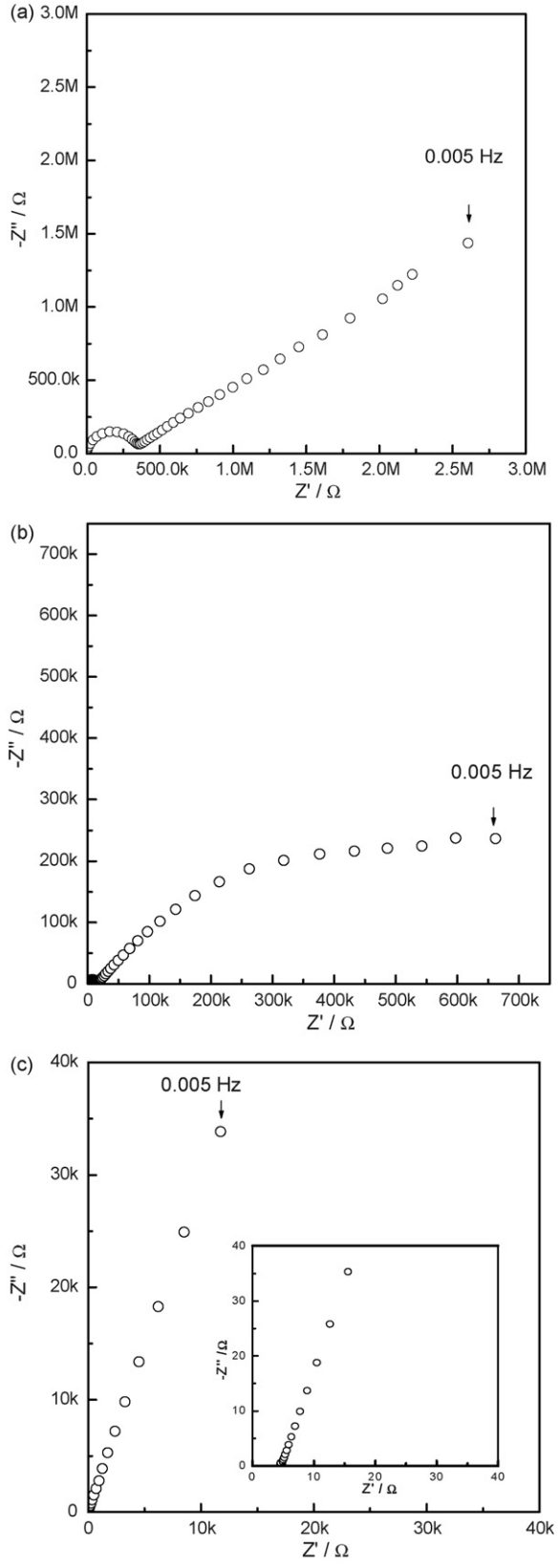

Fig. 5. EIS of SS/polymer electrolyte/SS cell at 25 °C for membrane (a) without organic plasticizer, (b) with 40 wt.% EC/DMC and (c) with 40 wt.% 1 M $LiPF_6$ in EC:DMC = 1:1, respectively. All of the membranes contain 3 wt.% organophilic MMT. Symbols Z' and Z'' refer to the real component and the imaginary component.

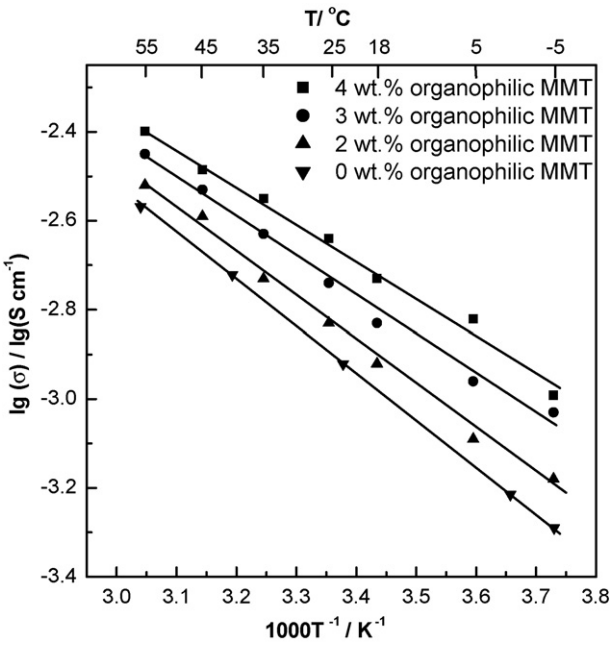

Fig. 6. Temperature dependence of ionic conductivity of GPEs with and without organophilic MMT filler. Continuous lines represent the fitted Arrhenius dependences.

this work based upon their boiling point, viscosity, and dielectric constant [27]. The corresponding liquid electrolyte (1 M $LiPF_6$ in EC:DMC = 1:1) has an ionic conductivity at around 11.5 mS cm^{-1} at RT. The nanocomposite polymer electrolytes with exfoliated organophilic MMT show relatively low ionic conductivity, which is about 1.6×10^{-8} and 3.5×10^{-7} S cm^{-1} for the cases in Fig. 5a and b, respectively. Interestingly, the GPE, which was made with 1 M $LiPF_6$ in EC:DMC, has comparatively high ionic conductivity (about 2×10^{-3} S cm^{-1}). The GPE (Fig. 5c) has the same content of organophilic MMT with other two samples. The result indicates that the contribution to the ionic conduction from the residual cations in clays can be ignored in GPEs. The ionic conductivities of GPEs decrease to some extent compared with that of the corresponding liquid electrolyte, which were found in the range of 1 mS cm^{-1} at RT. The GPEs with exfoliated organophilic MMT have higher ionic conductivity than that of GPEs without the filler (see Fig. 6). The solvent uptake and ionic conductivity increase as the organophilic MMT content increasing in GPEs. Clearly, the addition of MMT has an obvious effect on the enhancing of ionic conductivity. It is well known electrolytes with a high dielectric constant and low viscosity can yield very high ion transport [28,29]. The reported highly ion transportation across the interface between the polymer and inorganic filler particles also could be attributed to the high ionic conductivity [11,30]. In this case, the electronegative silicate platelets in the nanocomposite with high dielectric constant could help to dissolve electrolyte salt ($LiPF_6$), and then increase the ion conduction. However, it is found that the polymer clay nanocomposite film becomes brittle when the organophilic MMT content exceeds 5 wt.%. It is difficult for a brittle film to be used in batteries fabrication, so the ratio of organophilic MMT to PVDF-HFP should be controlled less than 5 wt.%.

Fig. 6 also depicts the relationship between the GPEs ionic conductivity and the temperature. The GPEs samples contain 0, 2, 3, and 4 wt.% organophilic MMT, respectively. The solvent uptakes were fixed at about 40 wt.% in these GPEs. All electrolyte systems in this figure showed similar temperature dependence, which suggests that the conductivity is thermally activated. From these data, the activation energy (E_0) for the movement of Li^+ ions in GPEs can be calculated by using the following Arrhenius expression:

$$\sigma = \sigma_0 \exp\left(\frac{-E_0}{RT}\right) \quad (3)$$

where σ_0 is a pre-exponential factor which may be related to ion mobility and ion association. E_0 is the activation energy.

The activation energy values E_0 calculated from Eq. (3) are 28.8, 19.3, 17.0, and 16.1 kJ mol^{-1} for GPEs with 0, 2, 3, and 4 wt.% organophilic MMT (error <5%), respectively. The result suggests that the exfoliated organophilic MMT have significant effect on the ion transportation activation energy, which is related to the ionic conductivity. GPEs show nearly unchanged ionic conductivity when they were shelved at high temperature (about 60 °C) for a long time. The results indicate that the polymer electrolyte containing exfoliated organophilic MMT has high structural stability and solvent maintaining capability.

Recently, polymer electrolytes with high cationic transfer number (t_{Li^+} near to 1) have been reported, but their ionic conductivity is not high enough for the practical applications in lithium or lithium ion batteries [19,31,32]. The effect of the fillers on the electrochemical behavior of the obtained polymer/clay nanocomposites, especially the cationic transference number, has been studied in this work. Examples of the typical steady-state currents obtained on different GPEs samples are presented in Fig. 7. According to the method proposed by Vincent [20] the Li^+ transference number values were estimated to be 0.363, 0.565, and 0.643 for GPEs with 0, 2, and 4 wt.% organophilic MMT, respectively. A general trend of increasing of t_{Li^+} with increasing organophilic MMT content was noted in all of the data. The result illustrates that the electronegative platelets of silicate has an important role on the cation transportation. By comparison with other polymer electrolytes, the polymer electrolyte based on polymer/clay nanocomposites in this work shows relative high cationic transference number [2,9].

In a lithium battery, not only the bulk resistance of the electrolyte but also the interfacial resistance between the electrolyte and electrodes contribute to the total resistance of the battery. The interface resistance corresponds to the compatibility of polymer electrolyte with the electrode material (Li metal in this case) and is an important factor in the use of a polymer electrolyte in the electrochemical devices. The interfacial resistance in a Li/GPEs/Li symmetric cell was evaluated under the open circuit condition by measuring its ac impedance response. The result impedance spectra in the Cole–Cole form as a function of time are presented in Fig. 8. The bulk resistance (R_b) of the GPE is almost a constant value (about 8 Ω). The interface resistance (R_i) due to the passivation layer continuously increases with time until a stable state obtained (from 34 to 57 Ω). The value of R_i due to the passivation layer between lithium and GPEs is very small. The result illustrates that GPEs has a stable interface with the lithium electrode during the storage period.

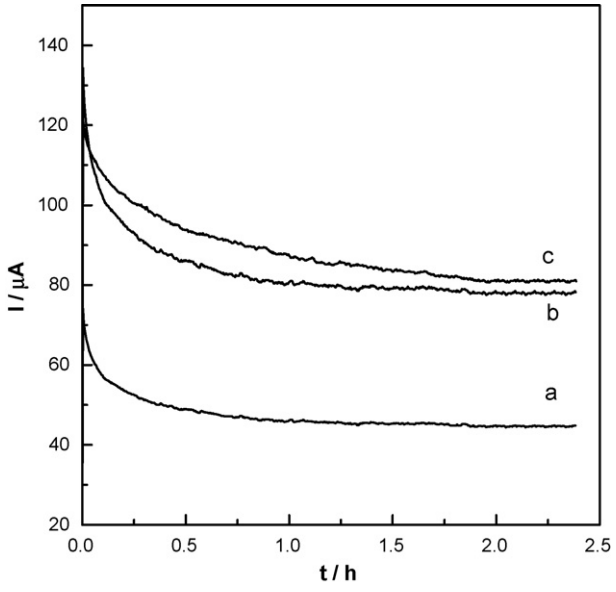

Fig. 7. Plot of current vs. time of the Li/GPE/Li cell polarized with 10 mV after 24 h of storage at RT for GPEs with (a) 0, (b) 2, (c) 4 wt.% organophilic MMT containing 60 wt.% 1 M $LiPF_6$ EC/DMC. The thickness of the polymer electrolyte membranes is about 200 μm. Parameters obtained for Li^+ transport number calculation: (a) I_s = 45.1 μA, R_b = 19.4 Ω, R_{i0} = 130.6 Ω, R_{is} = 168.5 Ω (t_{Li^+} = 0.36); (b) I_s = 78.1 μA, R_b = 13.9 Ω, R_{i0} = 74.1 Ω, R_{is} = 103.5 Ω (t_{Li^+} = 0.57); (c) I_s = 80.9 μA, R_b = 10.5 Ω, R_{i0} = 83.6 Ω, R_{is} = 107.3 Ω (t_{Li^+} = 0.64). The symbols have their usual meanings as shown in Ref. [20].

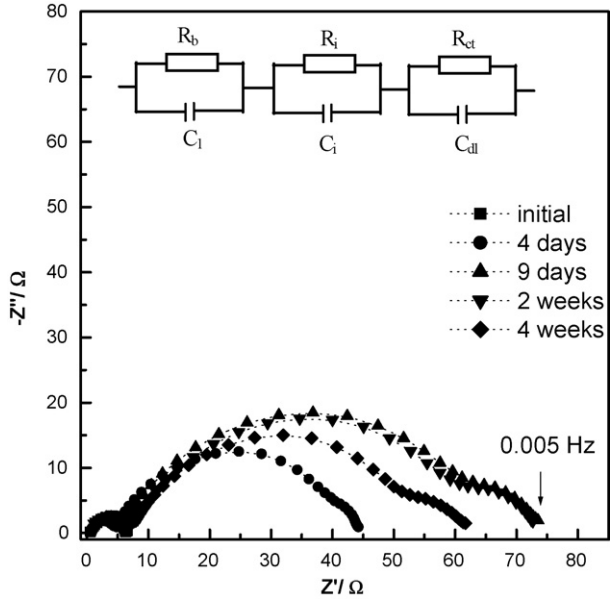

Fig. 8. Cole–Cole plots of the Li/GPE/Li cell as a function of time at room temperature. The GPE has the same composition as in Fig. 5c. The equivalent circuit is shown in the inset. R_b, R_i, and R_{ct} represent the resistance of bulk electrolyte, interface between electrolyte and electrode, and charger transfer; C_1, C_f and C_{dl} represent the bulk electrolyte, interface and double-layer capacitance, respectively.

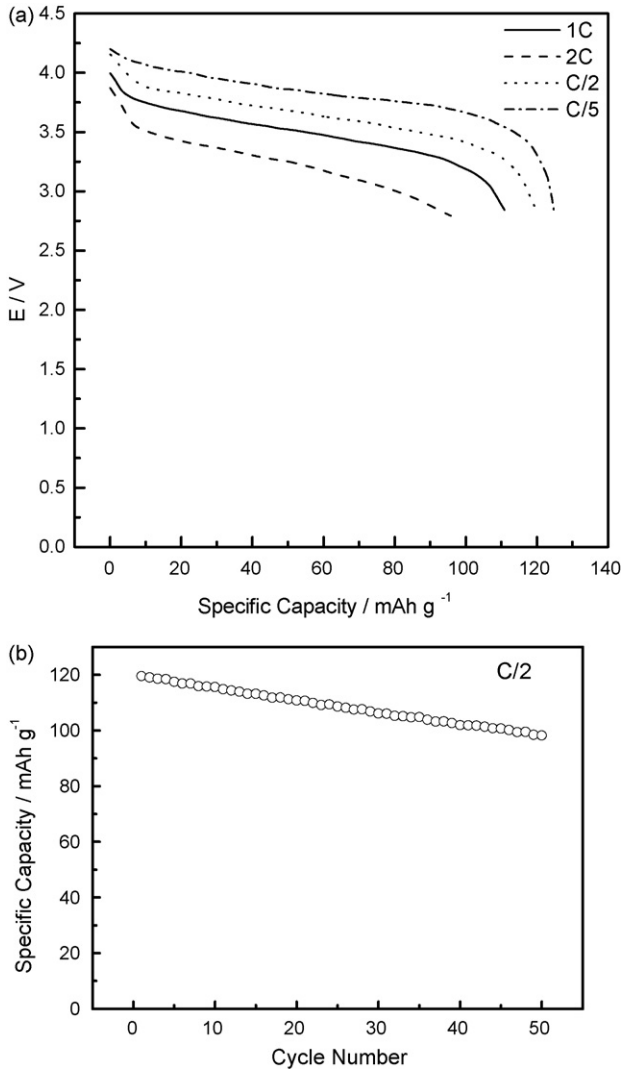

Fig. 9. Discharge curve at various discharge rates for Li-ion polymer battery (MCMB/GPEs/$LiCoO_2$) which used PVDF-HFP nanocomposite electrolytes. The GPE has the same composition as in Fig. 5c. Inset: discharge capacity as a function of cycle number of Li-ion polymer battery based on PVDF-HFP nanocomposite electrolyte at 0.5 C rate at RT. Liquid electrolyte used to prepare the GPEs is 1 M $LiPF_6$ in EC:DMC = 1:1.

According to the above results on electrolyte uptake, ionic conductivity and cation transference number, the prepared GPEs exhibit superior potential in the rechargeable lithium batteries application. Among these polymer electrolytes, the GPE with 3 wt.% organophilic MMT displays simultaneously high ionic conductivity, good mechanical strength and a wide electrochemical window. It was therefore used to make demo cells (MCMB/GPE/$LiCoO_2$) for the performance test. The assembled cells were subjected to a preconditioning cycle with cutoff voltages of 4.2 V for the upper limit and 2.8 V for the lower limit at a constant current of 0.2 mA (about 0.1 C rate) before the repeated charge and discharge at higher rate. The rate capabilities of a demo cell at RT are presented in Fig. 9. It appears that a high-rate capability was realized for this type of electrolyte due to its high ionic conductivity. At the 1 C discharge rate, the cell can deliver about 89% of its 0.5 C capacity. Even at a high 2 C rate, the cell can still deliver about 74% of its 0.5 C capacity. The cell has worse high-rate capacity when using the GPE without exfoliated MMT as the separator. The discharge capacity decreases when the charge/discharge rate increases, which is a natural behavior of Li-ion battery. The cycle-ability of the MCMB/GPE/$LiCoO_2$ cell at the C/2 rate between 2.8 and 4.2 V at RT is presented in Fig. 9b also. The cell was charged at 0.1 C rate and discharged at 0.5 C rate. At the first few cycles, the cell has the capacity about 120 mAh g^{-1}. Then the capacity decreases slowly during cycling and retains about 85% of the initial discharge capacity after 50 cycles, indicating the interfaces between GPEs and electrodes in the battery are stable under active conditions. From these results, it can be concluded that the PVDF-HFP based nanocomposite polymer electrolyte has an enough potential for the use in Li-ion polymer battery. However, a decrease of the discharge capacity was often found in this battery, which is mainly caused from the delamination between the polymer electrolytes and the electrodes (especially the anode). This behavior could be attributed to the high polarity solvent with lower adhesion property, which is used to prepare the electrolyte film. The gaseous byproducts during the charge–discharge process can also decrease the behavior of Li-ion polymer battery, such as the cycle life [33]. For practical application of this polymer electrolyte, much more attention should be paid to the interfacial adhesion between polymer electrolyte film and electrodes in the future.

4. Conclusions

This work reported a polymer electrolyte based on polymer/clay nanocomposites. In order to avoid the "pillar effect" in the intercalated nanocomposite, the exfoliated MMT clays were used. The polymer/clay nanocomposite materials exhibit good film formation, solvent maintaining capability, and dimensional stability. After gelling with liquid electrolyte solution (for example, 1 M $LiPF_6$ in EC:DMC), the obtained GPEs have high ionic conductivity (1–2.5 mS cm^{-1}) with high cationic transfer number at RT, which strongly depends on the content of organophilic MMT. The enhanced of electrochemical properties could be attributed to the distinctive characteristic of the well-dispersed silicate layers. The polymer electrolyte developed in this study shows the promise for the application in rechargeable lithium batteries.

Acknowledgments

The work was supported by the National Natural Science foundation of China. Constructive comments of two anonymous referees considerably improved the quality of the manuscript.

References

[1] W.H. Meyer, Adv. Mater. 10 (1998) 439.
[2] F.B. Dias, L. Plomp, J.B.J. Veldhuis, J. Power Sources 88 (2000) 169.
[3] A.D. Pasquier, P.C. Warren, D. Culver, A.S. Gozdz, G.G. Amatucci, J.-M. Tarascon, Solid State Ionics 135 (2000) 249.
[4] W. Henderson, N. Brooks, V.G. Young Jr., J. Am. Chem. Soc. 125 (2003) 12098.

[5] S.W. Choi, S.M. Jo, W.S. Lee, Y.-R. Kim, Adv. Mater. 15 (2003) 2027.
[6] M. Wang, L. Qi, F. Zhao, S. Dong, J. Power Sources 139 (2005) 223.
[7] K. Xu, Chem. Rev. 104 (2004) 4303.
[8] F. Croce, G.B. Appetecchi, L. Persi, B. Scrosati, Nature 394 (1998) 456.
[9] P. Mustarelli, E. Quartarone, C. Tomasi, A. Magistris, Solid State Ionics 135 (2000) 81.
[10] J. Travas-Sejdic, R. Steiner, J. Desilvestro, P. Pickering, Electrochim. Acta 46 (2001) 1461.
[11] M. Wang, F. Zhao, S. Dong, J. Phys. Chem. B 108 (2004) 1365.
[12] T. Abe, N. Gu, Y. Iriyama, Z. Ogumi, J. Fluorine Chem. 123 (2003) 279.
[13] E.P. Giannelis, Adv. Mater. 8 (1996) 29.
[14] P. Jeevanandam, S. Vasudevan, J. Phys. Chem. B 102 (1998) 4753.
[15] K. Yano, A. Usuki, A. Okada, J. Polym. Sci. Part A 35 (1997) 2289.
[16] M. Jacob, E. Hackett, E.P. Giannelis, J. Mater. Chem. 13 (2003) 1.
[17] J. Yeh, S. Lion, C. Liu, C. Cheng, Y. Chang, K. Lee, Chem. Mater. 14 (2002) 154.
[18] M. Wang, F. Zhao, Z. Guo, S. Dong, Electrochim. Acta 49 (2004) 3595.
[19] H.J. Walls, M.W. Riley, R.R. Singhal, R.J. Spontak, P.S. Fedkiw, S.A. Khan, Adv. Funct. Mater. 13 (2003) 710.
[20] P.G. Bruce, C.A. Vincent, J. Electroanal. Chem. 225 (1987) 1.
[21] M. Yoonessi, H. Toghiani, W.L. Kingery, C.U. Pittman Jr., Macromolecules 37 (2004) 2511.
[22] T. Lan, P.D. Kaviratna, T.J. Pinnavaia, Chem. Mater. 7 (1995) 2144.
[23] J. Saunier, F. Alloin, J.Y. Sanchez, B. Barrière, J. Polym. Sci. Part B 42 (2004) 532.
[24] J.R. Macdonald, J. Chem. Phys. 61 (1974) 3977.
[25] W.H. Mulder, J.H. Sluyters, Electrochim. Acta 33 (1988) 303.
[26] S. Abbrent, J. Lindgren, J. Tegenfeldt, J. Furneaux, A. Wendsjö, J. Electrochem. Soc. 146 (1999) 3145.
[27] G.E. Blomgren, in: D. Aurbach (Ed.), Nonaquous Electrolyte, Marcel Dekker, Inc., New York, 1999, pp. 53–81.
[28] J. Song, Y. Wang, C. Wan, J. Power Sources 77 (1999) 183.
[29] K. Hayamizu, Y. Aihara, S. Arai, C.G. Martinez, J. Phys. Chem. B 103 (1999) 519.
[30] T. Abe, M. Ohtsuka, F. Sagame, Y. Iriyama, Z. Ogumi, J. Electrochem. Soc. 151 (2004) A1950.
[31] M.W. Riley, P.S. Fedkiw, S.A. Khan, J. Electrochem. Soc. 149 (2002) A667.
[32] P. Aranda, Y. Mosqueda, E. Pérez-Cappe, E. Ruiz-Hitzky, J. Polym. Sci. B 41 (2003) 3249.
[33] D. Aurbach, J. Power Sources 89 (2000) 206.